

# Dispersive analysis of the $\pi^+\pi^-$ production at the CMD3 experiment and the compatibility with muon pair production measurement by KLOE2 and the pion form factor by JLAB

Dimitrios Petrellis and Vladimír Šauli<sup>1</sup>

<sup>1</sup>*Department of Theoretical Physics, Institute of Nuclear Physics Rez near Prague, CAS, Czech Republic*

The spectral function of the charged pion form factor was extracted from two data sets. The difference between the two sets is based on the presence or absence of the recent measurement of the  $\pi^+\pi^-$  production by CMD3. Although the CMD3 data are largely incompatible with other recent measurements, it was found to provide no excess when used for analytical continuation to spacelike region. Consequently, there is evidence for incompatibility when it is compared to the spacelike pion form factor obtained by the JLAB- $\pi$  experiment. Furthermore, the extracted pionic spectral function was used to obtain the QED running charge. It was then compared with the KLOE2 experiment for radiative return  $\mu^-\mu^+$  production at  $\omega/\rho$  meson energy. For this purpose the hadronic vacuum polarization has been extracted from exclusive hadronic productions in  $e^+e^-$  collisions via the dispersion relation using combined data with and without the CMD3 data set included in.

PACS numbers: 11.55.Fv, 13.66.Jn, 13.66.De, 13.66.Bc, 14.40.Be

## I. INTRODUCTION

The precise determination of Hadronic Vacuum Polarization (HVP) represents an important issue for comparison between theory and experiment. It is the source of the largest systematic uncertainties in the determination of muonic magnetic moment [1–3]. To this end, the optical theorem and a few other non-perturbative methods [5, 6] can be used to calculate the muon anomalous magnetic moment,  $a_\mu$ .

A plethora of precise experiments conducted over the last two decades at BABAR, Belle, BESS, and by the SND/CMD collaborations provided data on exclusive processes  $e^+e^- \rightarrow \text{hadrons}$  that are needed to determine the HVP. However, regarding the most important two-particle channel,  $e^+e^- \rightarrow \pi^+\pi^-$ , the associated data exhibit significant mutual incompatibility when different experiments are compared. In addition, based on the new generation experimental setup CMD3, the experimental group in Novosibirsk provided in [4] the measured data on the charged pion pair production cross section that deviates most significantly in the  $\rho$  resonance region. This suggests an unknown systematic error presented in measurement. While the difference in measured cross sections below  $1\text{GeV}$  was already significant (e.g., compare BABAR and BESS3 data), the difference now exceeds ten standard deviations at the  $\rho$  meson peak. While the mutual incompatibility of the pion electroproduction cross section is striking, it is interesting to see to what degree this incompatibility is reflected in related experiments. Naturally, one can ask if there is a chance to discriminate the quality of the data by using the knowledge from other related experiments.

The main motivation of the present work is to check how the aforementioned incompatibility affects the theoretical calculation of two related observables. First, within the use of assumed dispersion relation, we check the compatibility with the measured pion form factor at spacelike kinematics. For this purpose we extract the spectral function of the pion charge form factor, make analytical continuation and compare to the JLAB- $\pi$  measurements [7, 8]. As a second check of incompatibility influence, we extract HVP with and without CMD3 data and compare the theory and KLOE2 measurement[9] of the fine structure coupling constant. A third motivation is to correct the, albeit small, numerical error identified in the author's early attempts [10] on the HVP and the pion form factor extractions.

The paper is organized as follows: The next section provides the necessary theory for  $\sigma_{\mu\mu}$  for the KLOE 2004 measurement. The combination of data and error propagation is explained in section III. The preparation of the pion cross section for the HVP calculation is discussed in a separate section IV, where we describe the extraction of the spectral function. In this section, we also compare it to the JLAB- $\pi$  experiment. We compare calculated running QED couplings with the experiment in section V and draw conclusions in the final Section.

## II. $\sigma_{\mu\mu}$ FOR KLOE 2004

This section presents the theory and the comparison between the calculated cross section,  $\sigma_{\mu\mu} = \sigma(e^+e^- \rightarrow \mu^+\mu^-)$  and the precise measurement obtained by KLOE detector [11].

The integrated cross section, for which we adopt approximations and conventions given in [12], can be written in

the following way

$$\sigma(s) = \frac{4\pi C_t}{|1 - \Pi(s)|^2} \left[ \sigma_A(s) \left( 2 - \beta_\mu^2 \left( 1 - \frac{C_t^2}{3} \right) \right) + \sigma_B(s) \right], \quad (2.1)$$

where  $C_t$  stands for  $\cos(\theta_{min})$  with  $\theta_{min} = 50^\circ$  ( $\theta_{max} = 140^\circ$ ), which is the KLOE experimental cut on polar scattering angle between  $\mu^-$  and  $e^-$  particles and  $\beta_\mu = \sqrt{1 - 4m_\mu^2/s}$ . The function  $\sigma_A(s)$  is defined so that its angular dependence is identical to that of the Born cross section. The rest is unique can be written as follows:

$$\sigma_B(s) = -\frac{\alpha^3}{4\pi s} (1 - \beta_\mu^2) \ln \frac{1 + \beta_\mu}{1 - \beta_\mu}. \quad (2.2)$$

The main term,  $\sigma_A(s)$ , is listed completely in [12], collects all leading logs of Dirac and Pauli form factors and the known soft photon contributions for which we take  $\ln \frac{\Delta\epsilon}{\epsilon} = 0.05$  (15 MeV cut on c.m.s. soft photon energy at  $\phi$  peak). Let us mention that both  $\sigma_A$  as well as  $\sigma_B$  are slowly changing real valued functions and do not play a significant role in the observed interference effect.

The integral cross section formula is proportional to the square of the fine structure constant  $\alpha(s)$ , which reads

$$\alpha(s) = \frac{\alpha}{1 - \Pi(s)}, \quad (2.3)$$

with  $\alpha = \alpha(0) = 1/137.0359991390$  and where the polarization function  $\Pi(s) = \Pi_l(s) + \Pi_h(s)$  is composed of the leptonic  $l$  and the hadronic  $h$  part.

Purely QED contributions are well known from perturbation theory [12]. For completeness, we present the leptonic contribution to the vacuum polarization function here:

$$\Pi_l(s) = \frac{\alpha}{\pi} \Pi_1(s) + \left( \frac{\alpha}{\pi} \right)^2 \Pi_{2e}(s), \quad (2.4)$$

where one the loop contribution is

$$\begin{aligned} \Pi_1(s) &= \Pi_e(s) + \Pi_\mu(s) + \Pi_\tau(s); \\ \Pi_f(s) &= -5/9 - x_f/3 + f(x_f); f = e, \mu, \tau; \\ f(x_f) &= \frac{\beta_f}{6} (2 + x_f) \left( \ln \frac{1 + \beta_f}{1 - \beta_f} - i\pi \right) \Theta(1 - x_f) \\ &\quad + \frac{\beta_f}{3} (2 + x_f) \arctan \left( \frac{1}{\beta_f} \right) \Theta(x_f - 1), \end{aligned} \quad (2.5)$$

where  $\beta_f = \sqrt{|1 - x_f|}$  and  $x_f = 4m_f^2/s$ . Also the leading second order logarithmic term

$$\Pi_{2e}(s) = \frac{1}{4} \left( \ln \frac{s}{m_e^2} - i\pi \right) + \zeta(3) - 5/24, \quad (2.6)$$

is taken into account. For heavy quarks and large  $q^2$  we employ perturbation theory with the extra factor  $\alpha \rightarrow \alpha N_c e_q^2$  in the appropriate one-loop expression.

The HVP function  $\Pi_h$  is extracted from the total hadronic production  $\sigma_h = \sigma_{tot}(e^+e^- \rightarrow hadrons)$  by using the following dispersion relation [13, 14]:

$$\Pi_h(s) = \frac{s}{4\pi^2 \alpha} \int_{m_\pi^2}^{\infty} d\omega \frac{\sigma_h(\omega) \left[ \frac{\alpha}{\alpha(\omega)} \right]^2}{\omega - s + i\epsilon}. \quad (2.7)$$

The knowledge of this quantity is dependent upon a multitude of experimental measurements of the hadronic exclusive processes. i.e.

$$\sigma_h = \sum_i \sigma_{h_i}, \quad (2.8)$$

with  $i = \pi\pi, KK, \pi\pi\pi, \pi\gamma, \dots$  noting that the photons emitted from the final hadronic states count as well.

The expression (2.7) represents a nonlinear integral equation with a singular kernel. To date, several groups [15–17] have steadily collected necessary data on  $\sigma_h$  and continuously provided a fresh look at the  $\Pi_h$  line-shape. In our case, the experimental group (e.g. for experimental data BABAR, SND, BESS) provided the so-called bare cross section -i.e. with vacuum polarization extracted out by the experimental group itself, the combined data were unified (i.e., all made bare or with the polarization taken into account) to determine the inflated error, as defined below.

In what follows, we describe the determination of  $\sigma_h$  in our case. To this point, the narrow resonances, such as heavy quarkonia, have been substituted by their Breit-Wigner functions and PDG parameters. The inclusion of the remaining part of the total cross-section, denoted by  $d\sigma_h$ , is performed numerically and constitutes the core of the method. Since the kernel in Eq. (2.7) is singular, a straight use of experimental data to integrate the Eq. (2.7) would lead to uncontrolled numerical noise and loss of accuracy.

To control the principal value integration, we first construct an analytic fit of  $\sigma_h$  as the first step. Using this fit, we establish and determine the inflated error. This is a crucial step when dealing with combined datasets that have large systematic uncertainties. One advantage of our method is that it deals with unknown systematic errors of various experiments in a statistical manner. As a byproduct, we provide some fits of the data that can be used elsewhere. A known disadvantage of using fits, is that we may introduce unwanted structure. We are fully aware of this weakness and we do not draw strong conclusions based on the shapes of the functions used in our fitting procedure. On the other hand, the obtained spectral functions of the pion form factor suggest a complex non-perturbative structure rather than clear evidence of individual mesonic excitations.

### III. FIT FOR $\sigma_h$ AND THE INFLATED ERROR

Mutual incompatibilities in data originating from various experiments are indicative of systematic errors. The methods used to determine experimental cross sections differ greatly. Uncertainties can originate from the new, not yet widely used method (note, the luminosity is obtained from modern laser facilities used in CMD3 experiment), or from approximations made in the Initial State Radiation methods, or from uncertainties in determining Bhabha scattering, which is widely used to estimate the luminosity of electron and positron beams. Systematic uncertainties, whether recognized or of unknown origin, consequently complicate standard  $\chi^2$  analysis, when applied to combined data.

In the present paper the experimental error propagation is facilitated by the introduction of semi-stochastic inflated error (IE). When an inflated error  $\bar{\sigma}_I$ , is appropriately defined, it can serve as a partial accounting of systematic error, even when the error is not well-determined, in a statistical sense. Given the absence of a consensus definition in the existing literature, we propose a novel approach to define IE through the fit  $\sigma_{fit}$  of data  $\sigma_h$ : the inflated error  $\bar{\sigma}_I$  is defined such that we get exactly (by requirement)  $\chi_I^2 = 1$  in a theoretically allowed space of the cross sections  $\sigma_{fit}(E)$  and inflated error functions  $\bar{\sigma}_I(E)$  through minimization of the following quantity

$$\chi_c^2 = \sum_j \frac{[\sigma_{h,c}(E_j) - \sigma_{fit,c}(E_j)]^2}{\bar{\sigma}_{I,c}^2(E_j)}. \quad (3.1)$$

where  $c$  stands for a given hadron production channel and  $E_j$  is the total energy of positron-electron pair.

In other words, we naively assume that the systematic errors of sufficiently independent experiments can be considered as additional noise. Since the introduced IE replaces the covariance error matrices  $\sigma_{jk}^{stat}$  of a single experiment, the following condition

$$\sigma_{jk}^{stat} \delta_{jk} < \bar{\sigma}_I(E_j) \quad (3.2)$$

should be applied to account for the systematic error in the statistical sample of the combined data for given process. Inequality (3.2) ensures that the inflated error can be taken equal to the statistical error when a single experiment is considered. Ideally, we should compare data with similar statistical errors to avoid proliferating experiments with low statistics. Otherwise, we may undervalue high-quality data, or, conversely, we may waste good data. The latter can occur when excessive filtering according to the condition (3.2) is used. To avoid wasting data in a non-ideal case, the IE can always be chosen larger, especially if its size is sufficient for the intended purpose. In this paper, we follow this approach and try to avoid excessive filtering.

A simplified choice is used and we assume normal distribution for inflated errors

$$\bar{\sigma}_{I,c}(E) = N_c \sqrt{\sigma_{fit,c}(E)}, \quad (3.3)$$

with channel (c) dependent, but energy-independent constant  $N_c$ .

#### IV. DISPERSION RELATION FOR THE PION ELECTROMAGNETIC CHARGE FORM FACTOR AND THE $\pi\pi$ CONTRIBUTION TO $\sigma_h$

Determining the cross section of the process  $e^+e^- \rightarrow \pi^+\pi^-$  cross section is of central importance. It provides non-perturbative information about the distribution of quarks and gluons inside the lightest hadron. Through the dispersion relation for HVP, it also provides significant (75 %) contribution to the muon anomalous magnetic moment.

The pion electromagnetic form factor  $F$  is defined by the matrix element

$$\langle \pi^+(p_+) | J^\mu | \pi^-(p_-) \rangle = (p_+ + p_-)^\mu F(q^2) \quad (4.1)$$

where the momentum  $q = p_- - p_+$ . For the production process  $q^2 > 4m_\pi^2 > 0$ , while for the spacelike electromagnetic form factor the kinematics  $q^2 < 0$ . The first is measured in the production processes for which we have collected data, the later is measured in electron-pion scattering experiments [18] and pion production of nucleus (\*) [8, 19–21]. In the timelike region the modulus of the form factor appears in the measured hadronic cross section

$$\sigma_{\pi\pi}(s) = \frac{\alpha^2(s)\pi\beta^3}{3s} F^2(s). \quad (4.2)$$

where  $s = q^2$ . It was a conventional habit that some experimental groups published the so called bare cross section  $\sigma^B$  with HVP removed, i.e.

$$\sigma^B(q) = [\alpha(0)/\alpha(q^2)]^2 \sigma(q) \quad (4.3)$$

where HVP was extracted on the basis of contemporary knowledge.

In this work, however, we distinguish two form factors, the standard one  $F$ , and the full one  $F^F$ , which is used when the HVP and other possible contributions are not removed from the cross section. In the single photon exchange approximation we define

$$F_F(s) = F(s)[\alpha(s)/\alpha(0)]^2 \quad (4.4)$$

for which we can write the

$$\sigma_{\pi\pi}(q) = \frac{\alpha^2\pi\beta^3}{3s} F_F^2(s). \quad (4.5)$$

It is not difficult to show that the full form factor  $F_F$  satisfies the dispersion relation

$$F_F(q) = \frac{1}{\pi} \int_{4m_\pi^2}^{\infty} \frac{\rho_F(a)}{q^2 - a + i\epsilon} da. \quad (4.6)$$

if the form factor  $F(s)$  obeys the same (with the replacement  $\rho_F(a) \rightarrow \rho(a)$ ). In this work we explicitly check that this is the case and the absorptive part of electromagnetic pion form factor,  $ImF = -\rho$ , is the sole quantity required to determine the function  $F$  in the timelike and the spacelike momenta as well. While the form factor  $F$  for the spacelike domain can be extracted from lattice simulations [22], however is noteworthy that, the  $ImF$  can be calculated from the QCD equations of motion [23], although with limited precision only. The fit for  $\rho_F$  is therefore employed here. Explicitly we use the following form:

$$\rho_F(a) = \Im \frac{1}{\mathcal{N}} \left[ \mathcal{W}_\rho^{GS}(a, m_\rho, \Gamma_\rho)(s) \frac{1 + c_\omega \mathcal{W}_\omega(a, m_\omega)}{1 + c_\omega} + c_\phi \mathcal{W}_\phi^{GS}(a) + \sum_i c_i \mathcal{W}_{GS}^i(a, m_i, \Gamma_i) \right]. \quad (4.7)$$

where  $c$  are real coefficients and two parametric function  $\mathcal{W}_i^{GS}$  and  $\mathcal{W}$  are listed in Appendix A.

This fit provides the inflated error determined by the constant  $N^2 = 0.49 \text{ nb}$  in Eq. (3.3). This fit is better than the one obtained previously in [24, 25] with the same data sample. Here we did not refer [10], e.g. due to the later identification of the error made in the code for the pion form factor evaluation. It has a tiny effect in the HVP evaluation considered in the paper [10], but it affects the spectral function considerably near the threshold. The error is corrected in this paper (see Appendix B).

The fitted parameters are listed in Table I. Reducing the IE further would require filtering (reducing the amount) in case of combined data. Since the achieved error is sufficient for determining error propagation, we will stop here. The obtained results suggest that the method of inflated error represents a meaningful method in many respects. Although extracting errors is a time-consuming task, the benefit of easy later use is significant.

On the other hand, despite the fact that a precise and smooth analytical fit is achieved, no strong conclusions should be drawn from the resulting fits of both sets of data. Note that half of the potential rho-meson excitations are ghosts, according to their negative couplings,  $c_i$ , and no such structure of our unitarized and analyticized Gounaris-Sakurai model could be meaningfully identified with radial rho mesonic excitation. These ghosts overlap normal sign broad resonances and are needed to shape the intrinsic non-perturbative effects reflected in the amplitude. Although negative couplings are accepted and used by experimental groups, there is no meaningful low energy theory to interpret them.

Perhaps more importantly, the CMD3 data-governed fit with standard statistical deviations has achieved a chi-squared value of 1, indicating that the dispersion relation (4.6) is excellently fulfilled in this case. There is no evidence of distortion of analyticity due to systematic experimental error. To this point, we are fully aware of the existing unitarity / analyticity bounds [26], which in principle can provide a fit-independent test of our analytical assumptions. However these methods are very difficult to apply to the timelike combined data considered here. To perform these analyses, we wrote two independent codes, one uses Python libraries and the other is based on repeated iterations. For the  $e^+e^- \rightarrow \pi\pi$  experimental cross section we have used the data collected by KLOE [27] by CMD/SND operating group [28], SND [29] detectors as well as the ISR method extracted data by BaBaR [30], and BESS-III [31].

For the data governed by the CMD3 experiment the  $n_{dof} = 209 + 45$ , where the latter number in the sum is for remaining data outside the CMD3 range. To show the error band, like in Fig. 2, the propagation of error was estimated within use of inflated error, where we took  $N^2 = 0.49$  nb. We calculated the individual inflated errors for each channel in the HVP calculation separately. However, this level of precision turns out to be unnecessary for correctly determining error propagation and for the purposes of this paper we use a common inflated error ( $N^2 = 1$  nb) when calculating the error bands in the figures presented

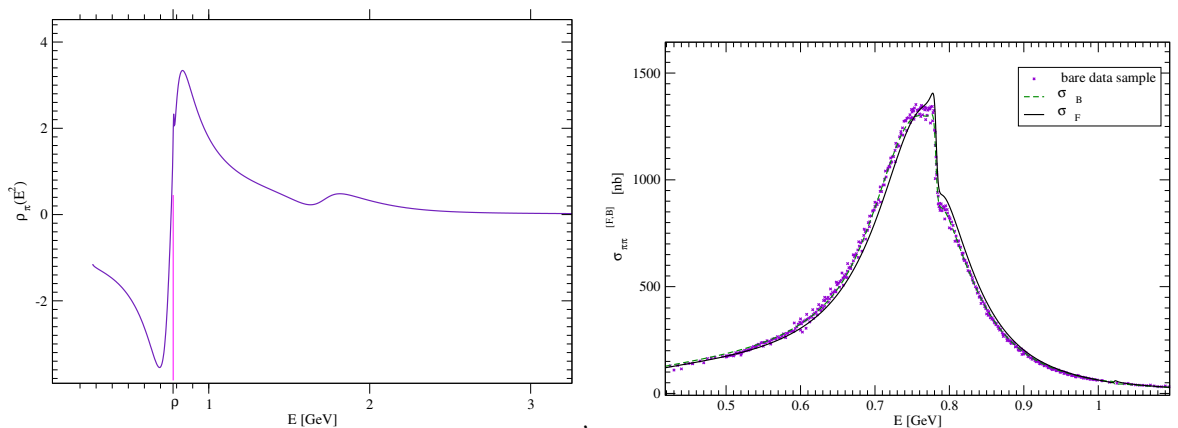


FIG. 1: Fits from the data Left: Spectral function of the QCD pion form factor  $F$  as extracted from data with CMD3 data. Right: Examples of selected cross sections as described in the text. The full cross section fit (solid) governed by CMD3 data is shown. The bare data-set with CMD3 data excluded and the associated fit of bare cross section (dashed) are shown as another example. Deviations are not shown for purpose of lines visibility.

The QCD fitted spectral function  $\rho_\pi$  is shown in Fig. 1. The set that do not contain CMD3 data was used in this case. Few examples of fits needed in our study are shown on the right panel. The difference between cross sections are due to vacuum polarization (absent for  $\sigma_B$ ) and due to the presence or absence of CMD3 data.

For further comparison of CMD3 and other datasets we refer to the original experimental paper [4].

### A. Results for the pion electromagnetic form factors

Using the obtained spectral functions the continuation to the spacelike region of momenta is straightforward. Continuations based on two extracted spectral functions are equally compatible with the experimental JLAB- $\pi$  data. This can be seen in Fig. 2, where comparison is made. In fact the CMD3 data-driven result for the electromagnetic form factor turns to be even slightly closer to the JLAB measurement. To determine the form factor, the statistical errors provided by CMD3 were used. While the inflated error was used to calculate the function  $F$  with the spectral function  $\rho$  based on the combined world data.

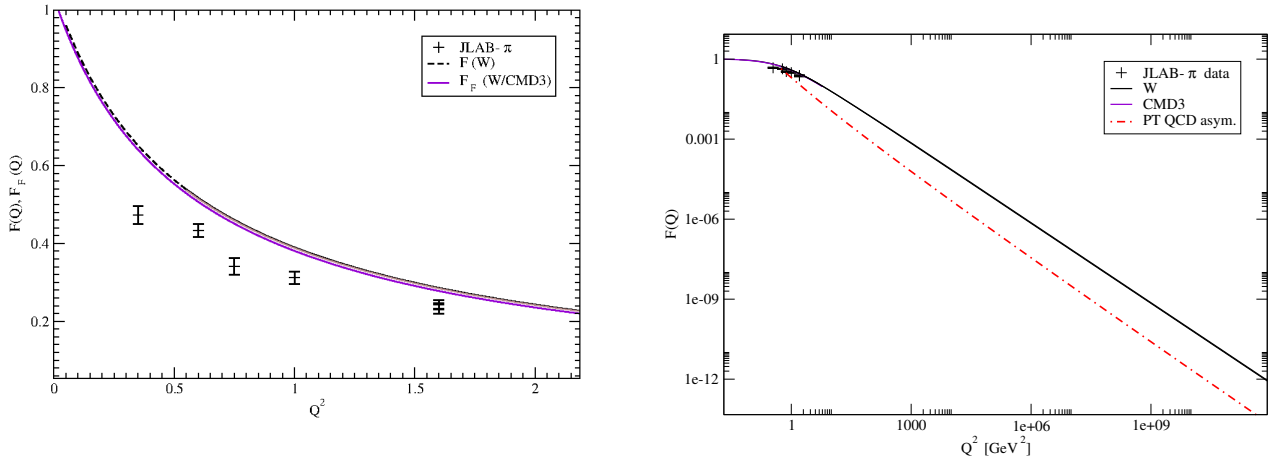


FIG. 2: Pion electromagnetic form factors continued from the timelike to the spacelike region. Left panel: Pure QCD pion form factor  $F(W)$  (dashed line) as obtained from world combined data without CMD3 data and the full form factors  $F_F$  as extracted from the data that includes CMD3 ( $F(W/CMD3)$ ) are shown. The border lines of the error band are shown for the later case. As it coincides with the later function  $F_F$ , the upper bound is shown only from the  $Q^2 = 0.5 GeV^2$  for the continued function  $F_F$ . Right panel: The form factors are compared to PT QCD asymptotics (dashed line)  $W$  (CMD3) label the function  $F$  continued from the world data without and within the CMD3 data included.

| fit      | CMD3+   |           |          | W (world without CMD3) |           |         |
|----------|---------|-----------|----------|------------------------|-----------|---------|
|          | m       | $\Gamma$  | c        | m                      | $\Gamma$  | c       |
| 0        | 0.7219  | 0.206     | -0.0518  | 0.6895                 | 0.113     | -0.036  |
| $\rho$   | 0.77453 | 0.15173   | 1        | 0.7754                 | 0.1565    | 1       |
| $\omega$ | 0.7821  | 0.0086099 | 0.001754 | 0.7817783              | 0.0087933 | 0.00169 |
| $\phi$   | 1.02181 | 0.00459   | 0.0007   | 1.02144                | 0.0042    | -0.0008 |
| 1        | 1.3832  | 0.291     | -0.0609  | 1.403                  | 0.206     | -0.0597 |
| 2        | 1.694   | 0.123     | 0.0161   | 1.684                  | 0.104     | 0.0196  |
| 3        | 2.45    | 0.66      | -0.0153  | 2.28                   | 0.49      | -0.017  |
| 4        | -       | -         | -        | 2.25                   | 0.1       | 0.0047  |

TABLE I: List of parameters for fits of pion electromagnetic form factor based on analyticized Gounaris-Sakurai model with CMD3 data (left part) and with world but without CMD3 data (right part). The CMD3+ fits is for the full form factor  $F_F$ , the group of three right columns is for the standard form factor  $F$  as majority of the world (W) data are for the bare cross section, where HVP has been removed by the the experimental groups themselves.

Normalization prefactors:  $\mathcal{N}_{CMD3+} = 0.8539$ ;  $\mathcal{N}_W = 0.8615$ .

Another interesting point is the question of agreement with perturbative PT QCD, where a known formula  $F \rightarrow \beta Q^{-2} \ln^{-1}(Q^2/\Lambda^2)$  has been obtained [33–36]. Assuming the validity of the dispersion relation 4.6, we find no evidence for the perturbation theory asymptotics. The deviation from a naive QCD asymptotic is not affected by the data set. Also the presence or absence of HVP are largely unimportant for this comparison. The PT form factor is compared with analytically continued form factors in the right Fig. 2. Actually, the asymptotic slopes of extracted form factors differ so significantly from PT form. There is no evidence of a PT log presence up to the TeV region of spacelike momenta.

Recall here, that in order to recover PT QCD asymptotics, one would need to get striking deviations from assumed analytical structure here. Till now, the experimental data do not support such a findings. More interestingly the unpublished JLAB data show possible evidence for opposite, observing  $Q^2 F(Q^2)$  takes constant value for  $Q$  at several  $GeV$  region.

## V. RESULTS FOR $\alpha_{QED}$ AT KLOE2

The QED running coupling is an observable that inversely depends on HVP. Two analytic fits for cross section  $\sigma_{\pi\pi}$  as described in the previous sections have been employed providing thus two different comparisons with KLOE2 data for running fine structure constant. In addition to the cross section  $\sigma_{\pi\pi}$ , we use the known fits [10, 24, 25] for the remaining exclusive channels, including  $K^+K^-$ ,  $K_L K_S$  and  $\pi\pi\pi$ , as well as subdominant  $\eta\gamma$  and  $\pi\gamma$  production cross sections in order to determine HVP through the formula (2.7). Up to  $\sigma_{\pi\pi}$ , all necessary fits to experimental data are summarized in [10] and are used without modification. Final states with four pions have also been included, while neglecting  $KK\pi$  and the other states with multiplicity higher than three. Furthermore, following the standard routine, the well-established vector charmonia and bottomonia have been included in  $\sigma_h$  via their BW forms with PDG averaged values.

The integral equation (2.7) was solved iteratively on a large numerical grid, ensuring that the numerical error is much smaller than the associated statistical and systematic deviations. The codes and resulting data are available to the public at pages of NPI institute. As in the case of the pion electromagnetic form factor, the numerics were enforced by using the so-called Hollinde trick when performing principal value integration.

We compare with the QED running coupling, which has been measured below 1 GeV by the the KLOE2 collaboration [9]. Two considered calculated results for the QED running coupling are compared in Fig. 3 for the KLOE2 accessible region.

Two determined HVP functions provide two distinct results for the running coupling. The incompatibility of the data sets with and without the CMD3 data is too small compared to the experimental errors of KLOE2 measurements. The same argument applies in the case of different results obtained by our method and by others [15, 16].

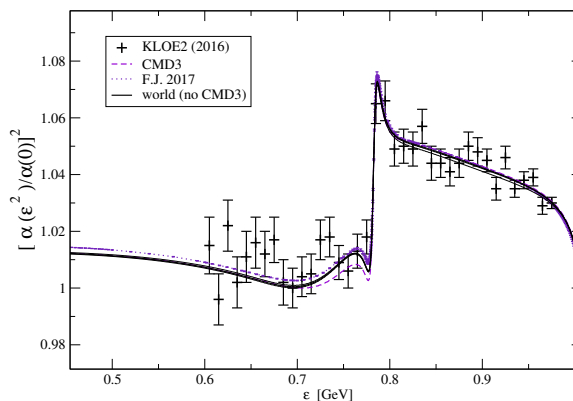


FIG. 3: Square of the fine structure constant as affected by the presence or absence of CMD3 data for the  $\sigma_{\pi\pi}$  cross section. The line labeled by F.J stands for HVP extractions made by [15].

## VI. CONCLUSION

The experimental data on  $e^+e^- \rightarrow hadrons$  suffers from relatively large systematic errors of unknown origin. The striking difference between the Babar and BESIII measurements was an extreme example before the CMD3 group published new data for two charged pions cross section. Despite the fact that the experimental points for  $\sigma_{\pi\pi}$  provided by the CMD3 group represent an outlier case among the other experiments, we have shown that the incompatibility imprints in related observables do not cause further tension between theory and experiments. This is true for the two cases of observables considered in our paper.

The first observable discussed is the elastic scattering of a pion on an electron (or proton). It is a matter of fact that the spacelike continuation of the CMD3-driven electromagnetic form factor is slightly closer to the experimental values. Additionally, we estimate the propagation of errors to a large spacelike  $Q$  and observe little chance of achieving the naive perturbative QCD limit. Assuming the form factor satisfies the usual dispersion relation, the function  $F$  in the deep spacelike region of momenta is unlikely to ever meet the PT QCD prediction.

Furthermore, the obtained spectral functions, together with the other considered spectral fits for hadronic production cross sections, was used to calculate the  $\sigma_{\mu\mu}$  cross section and the QED running charge in the time-like region of the momenta and compared with the 2004 KLOE  $\sigma_{\mu\mu}$  as well as with the 2016 KLOE2 measurement for the electromagnetic running charge. In this case it would require at least ten times better precision than the KLOE2 experiment to potentially detect incompatibility of the data. Similar comparisons as presented in our study can be a challenging task for future high-precision measurements.

### Appendix A: Details of the analytical fit

In this appendix we review the list of functions used in our constructions.

Particularly important is the form of the Gounaris-Sakurai dressed vector meson propagator, which is

$$\mathcal{W}^{GS} = \frac{m^2 + d(m)\Gamma/m}{M^2(s) - s - im\Gamma(s, m, \Gamma)}, \quad (\text{A1})$$

$$M^2(s) = m^2 \left[ 1 + \frac{\Gamma k^2(s)}{k^3(m)} (h(s) - h(m^2)) + \frac{\Gamma h'(m^2)}{k(m)} (m^2 - s) \right], \quad (\text{A2})$$

$$\begin{aligned} \Gamma(s, m, \Gamma) &= \Gamma \frac{m}{\sqrt{s}} \left[ \frac{L_2(s, m_\pi)}{L_2(m^2, m_\pi)} \right]^3, \\ L_2(s, m_\pi) &= \sqrt{s - 4m_\pi^2}, \end{aligned} \quad (\text{A3})$$

where we have defined following auxiliary functions:

$$h(s) = \frac{\beta(s)}{2} \ln \left( \frac{\sqrt{s} + 2k(s)}{2m_\pi} \right), \quad (\text{A4})$$

$$h'(m^2) = \frac{2m_\pi^2 h(m)}{m^4 \beta(m)} + \frac{2m_\pi^2}{\pi m^4 \beta(m)} + \frac{\beta(m)}{2\pi m^2}, \quad (\text{A5})$$

$$d(m) = \frac{4m_\pi^2}{m^2 \beta^3(m)} (3h(m) - 2/\pi) + \frac{1}{\pi \beta(m)}, \quad (\text{A6})$$

with the usual shorthand notation:

$$\beta(s) = \frac{L_2(s, m_\pi)}{\sqrt{s}}, \quad k(s) = \frac{L_2(s, m_\pi)}{2}, \quad (\text{A7})$$

used for the velocity and the two pion Lorentz invariant phase space factor.

The Breit-Wigner function for the narrow  $\omega$  meson was taken in the form:

$$\mathcal{W}_\omega = \frac{m_\omega^2}{m_\omega^2 - s - im_\omega \Gamma_\omega}. \quad (\text{A8})$$

### Appendix B: Holinde trick

To improve the principal value integration numerically we subtract (add) the exact zero from the original integral

$$\begin{aligned} \int_T^\infty dx \frac{f(x)}{y-x} &= \int_T^\infty dx \frac{f(x)(x+y) - f(y)2y}{y^2 - x^2} \\ &\quad + f(y) \ln \frac{1-T/y}{1+T/y} \end{aligned} \quad (\text{B1})$$

, which is the actual form used for discretization to the sum.

It is the term in the second line that has been neglected in the evaluation of the pion form factor in the unpublished paper [10]. (\*)

- 
- [1] G. Bennet et al., Phys. Rev. Lett. 89, 101804 (2002).
  - [2] K. Olive et al., Review of Particle Physics, The Muon Anomalous Magnetic Moment by A. Hoecker and B. Marciano, Chin. Phys. C 38, 090001 (2014).
  - [3] B. Abi et al., Phys. Rev. Lett. 126, 141801 (2021).
  - [4] CMD-3 Collaboration: F. V. Ignatov et al. Phys. Rev. D **109**, 112002 (2024).
  - [5] T. Hilger, M. Gomez-Rocha, A. Krassnigg, Eur. Phys. J. C 77, 625 (2017).
  - [6] T. Goecke, Ch. S. Fischer, R. Williams, Phys. Lett. **B** 704, 2011-217 (2011).
  - [7] Jefferson Lab collaboration, G. M. Huber et al., Phys. Rev. C 78 045203, (2008).
  - [8] Jefferson Lab collaboration, H. P. Blok et al., Phys. Rev. C 78, 045202 (2008).
  - [9] KLOE2 Collab. and F. Jegerlehner, Phys. Lett. B 767, 485–492 (2017).
  - [10] V. Sauli, unpublished, arXiv:1708.03616 .
  - [11] F. Ambrosino, et al.; Phys. Lett. B 608, 199-205 (2005).
  - [12] A. B. Arbuzov, et al.; JHEP 9710, 001 (1997).
  - [13] N. Cabibbo and R. Gatto, Phys. Rev. 224, N.5,1577-1595 (1961).
  - [14] S. Eidelman, F. Jegerlehner, Z. Phys. C67, 585-602 (1995).
  - [15] F. Jegerlehner, J. Phys. G 29, 101 (2003), the updated code is available at <http://www-com.physik.hu-berlin.de/~fjeger>
  - [16] The vacuum polarisation corrections used by Novosibirsk experiments (SND, CMD2, CMD3): <http://cmd.inp.nsk.su/~ignatov/vpl> .
  - [17] M. Davier, A. Hoecker, B. Malaescu, Z. Zhang, Eur. Phys. J. C71, 1515 (2011).
  - [18] NA7 collaboration, S. R. Amendolia et al., Phys. B 277,168 (1986)
  - [19] Jefferson Lab F(pi) collaboration, J. Volmer et al., Phys. Rev. Lett. 86 (2001) 1713–1716, (2001).
  - [20] Jefferson Lab F(pi)-2 collaboration, T. Horn et al., Phys. Rev. Lett. 97, 192001 (2006).
  - [21] Jefferson Lab F(pi) collaboration, V. Tadevosyan et al., Phys. Rev. C 75, 055205 (2007).
  - [22] X. Gao et al, Phys. Rev. D **104**, 11, 114515 (2021).
  - [23] V. Sauli, Phys. Rev. D **106** 3, (2022).
  - [24] V.Sauli, Acta Phys. Polon .Supp. 10 no.4, 1159-1164 (2017).
  - [25] V. Sauli, FCCP2017, EPJ Web Conf. 179, 01021 (2018).
  - [26] S. Simula and L. Vittorio, Phys. Rev. D **108**, 094013 (2023).
  - [27] A. Aloisio, et al (KLOE Collaboration), Phys. Lett. B 606, 12–24 (2005).
  - [28] V. M. Aulchenko, et al (CMD-2 Collaboration), JETP Lett. 82, 743-747 (2005); PismaZh. Eksp. Teor. Fiz. 82, 841-845 (2005).
  - [29] M.N.Achasov,et al, J. Exp. Theor. Phys. 103, 380-384 (2006); Zh. Eksp. Teor. Fiz. 130, 437-441 (2006).
  - [30] J. P. Lees (BABAR Collaboration), Phys. Rev. D 86, 032013 (2012).
  - [31] M. Ablikim, (BESIII Collaboration) Phys. Lett. B753, 629-638 (2016).
  - [32] Most important codes and data files are usually stored at the athor’s web page: <http://gemma.ujf.cas.cz/~sauli/papers.html>
  - [33] V. Chernyak and A.R. Zhitnisky, JETP Lett. 43, 510 (1977); Sov. J Nucl. Phys. 31, 544 (1980).
  - [34] G. Farrar and D. Jackson, Phys. Rev. Lett. 43, 246 (1979).
  - [35] G. P. Lepage and S. J. Brodsky, Phys. Lett. 87 B, 359 (1979); Phys. Rev. D 22, 2157 (1980).
  - [36] A. V. Efremov and A. V. Radyushkin, Phys. Lett. 94 B, 245 (1980).